A process-based framework for quantifying the atmospheric preconditioning of surface-triggered convection

Ahmed B. Tawfik[1] and Paul A. Dirmeyer[1]

Received 12 September 2013; revised 11 November 2013; accepted 13 November 2013.

[1] Here we introduce the heated condensation framework, which contains a suite of variables for isolating the atmospheric boundary state from local surface forcing. The buoyant condensation level (BCL) and buoyant mixing temperature (θ_{BM}) quantify the degree to which the atmosphere is preconditioned for moist convection and can be calculated for any time of day or year using standard vertical profiles of temperature and humidity. Unlike the lifted condensation level and convective inhibition, the BCL is constructed through incremental mixing from the surface rather than lifting a hypothetical parcel. In this regard, the BCL represents a conserved condensation level diagnostic inherent to a given profile. The BCL and θ_{BM} are shown to be applicable over a range of climate regimes and respond to synoptic and mesoscale forcings, illustrating its broader utility. A suite of variables relating the BCL directly to surface fluxes is also introduced. **Citation:** Tawfik, A. B., and P. A. Dirmeyer (2014), A process-based framework for quantifying the atmospheric preconditioning of surface-triggered convection, *Geophys. Res. Lett.*, *41*, doi:10.1002/2013GL057984.

1. Introduction

[2] The role of the land surface in triggering and amplifying precipitation has been the focus of recent research [e.g., *Zhang and Klein*, 2010; *Findell et al*., 2011; *Gentine et al*., 2013b; *Santanello et al*., 2013] reflecting the ability of soil moisture states to affect precipitation [*Fennessy and Shukla*, 1999; *Betts*, 2004]. This coupling has been most strongly identified over semiarid regions [*Guo et al*., 2006; *Koster et al*., 2006] due to greater flux sensitivity and variability [*Dirmeyer*, 2011]. Thus, the potential exists for improved seasonal predictability by better representation of soil moisture [*Guo et al*., 2011; *Koster et al*., 2011]. To better understand the impact of surface forcing on precipitation, atmospheric preconditioning (the synoptic background state) must be quantified in a manner physically consistent with land-boundary layer interactions.

[3] The growth of the planetary boundary layer (PBL) throughout the day is a function of the interplay between surface fluxes, the vertical profile of the overlaying atmosphere, and advection [*Betts*, 2000, 2009; *Berg and Stull*, 2004]. As the surface is heated by incident radiation, near-surface air becomes more buoyant. Rising air mixes upward, homogenizing the air within the growing PBL while entraining relatively dry air from the free troposphere [*Berg and Stull*, 2004; *Betts*, 2009]. This results in near-constant potential temperature and water vapor mixing ratio profiles and also serves to define the PBL height itself. Clouds may form if the top of the PBL is sufficiently cooled [*Gentine et al*., 2013a; *Zhang and Klein*, 2013], potentially producing precipitation [*Haiden*, 1997].

[4] Treating land-atmosphere interactions as a cascade of steps from the surface to the atmosphere allows the relative importance of different processes to be isolated [*Seneviratne et al*., 2010; *Santanello et al*., 2011]. Efforts have been made to derive metrics for quantifying these particular steps [*De Ridder*, 1997; *Findell and Eltahir*, 2003; *Ek and Holtslag*, 2004; *Santanello et al*., 2009; *van Heerwaarden et al*., 2010; *Ferguson et al*., 2012]. However, disentangling the large-scale forcing from the local land surface forcing has been particularly difficult [*Berg and Stull*, 2004; *Ferguson and Wood*, 2011]. *Findell and Eltahir* [2003] introduced a method using morning soundings that identifies certain regimes where the land surface may influence convective triggering. Although this method was robust over Illinois, *Ferguson and Wood* [2011] had to modify thresholds to be suitable globally when using remote sensing data. Other studies have quantified the free-tropospheric stability using temperature and specific humidity lapse rates above the PBL within the context of convective triggering [*De Ridder*, 1997; *Ek and Holtslag*, 2004; *Gentine et al*., 2013b]. This is typically done using a "jump" criterion in a single-column model where conserved fields (potential temperature and specific humidity) are perturbed at the top of the mixed layer mimicking the transition to the free troposphere. Conserved parcel metrics such as the lifted condensation level (LCL), the level of free convection (LFC), and convective inhibition (CIN) have also been used as diagnostics for identifying convective triggering [*Betts*, 2004; *Guichard et al*., 2004; *Zhang and Klein*, 2010; *Santanello et al*., 2011]. *Santanello et al*. [2011] showed that when the LCL is below the PBL depth, convection may occur providing a necessary but not sufficient condition for convective triggering. *Gentine et al*. [2013b] used the difference between the mixed layer and saturation equivalent potential temperature above the inversion to diagnose the difference between active and forced convections.

[5] These methods typically neglect the incremental growth of the PBL by one of two assumptions: (1) basing metrics on atmospheric states at arbitrary heights or (2) lifting a parcel from a certain height without allowing the parcel to mix with its surroundings. This is problematic especially on hourly timescales where LCL, LFC, and CIN are seen to vary

Additional supporting information may be found in the online version of this article.

[1]Center for Ocean-Land-Atmosphere Studies, George Mason University, Fairfax, Virginia, USA.

Corresponding author: A. B. Tawfik, Center for Ocean-Land-Atmosphere Studies, George Mason University, 4400 University Drive, Mail Stop 6C5 Fairfax, VA 22030, USA. (abtawfik@cola.iges.org)

0094-8276/14/10.1002/2013GL057984

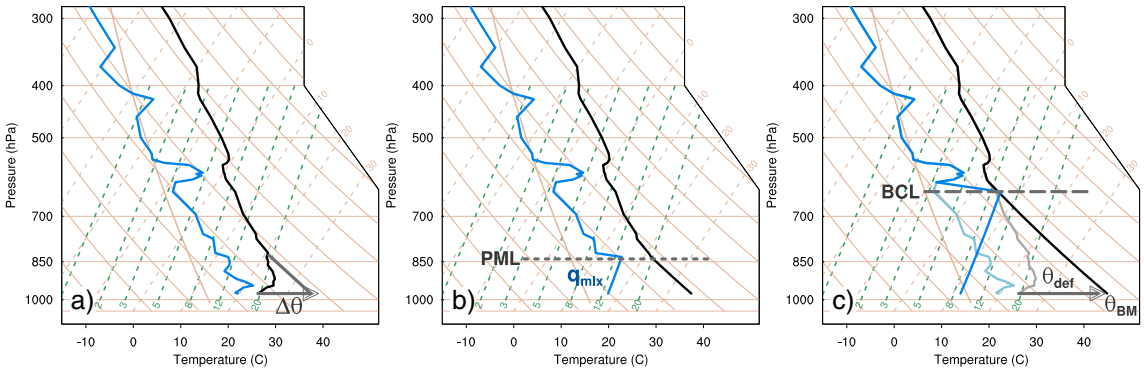

Figure 1. Thermodynamic profiles (e.g., skewT-logP diagrams) of temperature (black) and dew point temperature (blue) illustrating the steps for calculating the buoyant condensation level (BCL), buoyant mixing temperature (θ_{BM}), and mixed layer specific humidity (q_{mix}). Dashed green lines represent constant mixing ratio lines; dashed tan lines represent isotherms; and solid tan lines are dry adiabats. (a) The first step where θ_{2m} is perturbed by some increment, $\Delta\theta$. (b) The height, the potential mixed level (PML), where the perturbed surface parcel ($\theta_{2m}+\Delta\theta$) is neutrally buoyant and the humidity profile is mixed from the PML to the surface. (c) The θ_{2m} is perturbed until saturation occurs at the PML, and the level is identified as the BCL. The total potential temperature increment is θ_{def} which is necessary to reach θ_{BM} from the initial θ_{2m}. Faint blue and grey lines in Figure 1c refer to the unperturbed profile shown in Figure 1a as a reference.

substantially throughout the day [*Guichard et al.*, 2004; *Betts*, 2009], making it difficult for such metrics to identify a representative atmospheric background state with respect to convection.

[6] Here we introduce a new diagnostic framework, the heated condensation framework (HCF), which defines the buoyant condensation level (BCL) and the buoyant mixing potential temperature (θ_{BM}). These two variables quantify how conditioned the atmosphere is to moist free convection due to surface heating. The HCF variables are calculated using standard meteorological soundings (specific humidity and temperature profiles) and may be calculated for any time of day. The framework produces a suite of other quantities that provide insight into the conditions necessary for triggering convection, but the primary focus here will be on variables that quantify the atmospheric background state (e.g., the BCL and θ_{BM}) with brief mention of how to calculate HCF variables related to surface fluxes. These HCF surface flux variables will be more thoroughly explored in a subsequent paper.

2. Heated Condensation Framework

[7] The BCL is defined as the level at which saturation would occur through buoyant mixing alone due to sensible heating from the surface. Alternatively, the BCL is the height the growing PBL needs to reach for saturation to occur without the addition or removal of moisture from the column. To find the BCL, a hypothetical boundary layer is constructed using the vertical profiles of potential temperature, θ, and specific humidity, q. This is done in four steps illustrated by the thermodynamic profiles in Figure 1: (1) Increase the near-surface potential temperature (θ_{2m}) by a small increment, $\Delta\theta$ (Figure 1a). (2) Find the height where the perturbed near-surface parcel ($\theta_{2m}+\Delta\theta$) is neutrally buoyant (Figure 1b). (3) Mix the specific humidity profile from the surface to the level of neutral buoyancy returning a constant mixed layer humidity, q_{mix} (Figure 1b). (4) Upon mixing, check if saturation occurs at the top of the potential mixed level (PML) by comparing q_{mix} and the saturation specific humidity at the PML, $q^*(\theta_{pml})$. The sequence is repeated until saturation occurs (Figure 1c). Note that the BCL is a special case of the PML when saturation is reached (e.g., $q^*(\theta_{pml}) - q_{mix} = 0$), where the sum of all $\Delta\theta$ increments required to attain the BCL is the total energy deficit, θ_{def} (Figure 1c). Unlike parcel-derived metrics (LCL, LFC, convective available potential energy, and CIN) that change for a given profile depending on the parcel selected for lifting, the BCL is an inherent property of a given profile that does not vary unless the temperature and humidity profiles change. This makes the BCL height independent from the initial θ_{2m} and is therefore insensitive to the starting temperature (e.g., time of day) as long as the q and T profiles do not change.

[8] Other useful quantities can also be derived within this framework. Specifically, the buoyant mixing potential temperature, θ_{BM}, identifies the near-surface potential temperature required to attain the BCL height ($\theta_{BM} = \theta_{2m} + \theta_{def}$). Before the BCL height is reached (step 4; Figure 1b), a moisture deficit at the top of the potential mixed layer (PML) can be calculated ($q_{def} = q^*(\theta_{pml}) - q_{mix}$). The θ_{def} and q_{def} are both easily translated into time integrated surface flux units. For example, multiplying q_{def} by the column density (ρ_h) of the potential mixed level returns the amount of moisture (either through evapotranspiration or advection) needed to be injected into the PML for saturation to occur at a given potential temperature. Similarly, θ_{def} multiplied by the specific heat capacity (c_p) and mean column density (ρ_h) returns the necessary sensible heat energy. Therefore, during each $\Delta\theta$ increment, the amount of heat input ($c_p\rho_h\Delta\theta$) and moisture input ($\rho_h q_{def}$) necessary for saturation can be quantified.

3. Data

3.1. Integrated Global Radiosonde Archive

[9] Vertical profiles of temperature and humidity are provided by the Integrated Global Radiosonde Archive [IGRA; *Durre et al.*, 2006]. The IGRA is a global quality-controlled sounding data set with the greatest spatial and temporal coverage over the United States and Europe typically measuring at 0000 UTC and 1200 UTC. Here we focus on the continental United States (23–50°N and 130–66°W) with data from

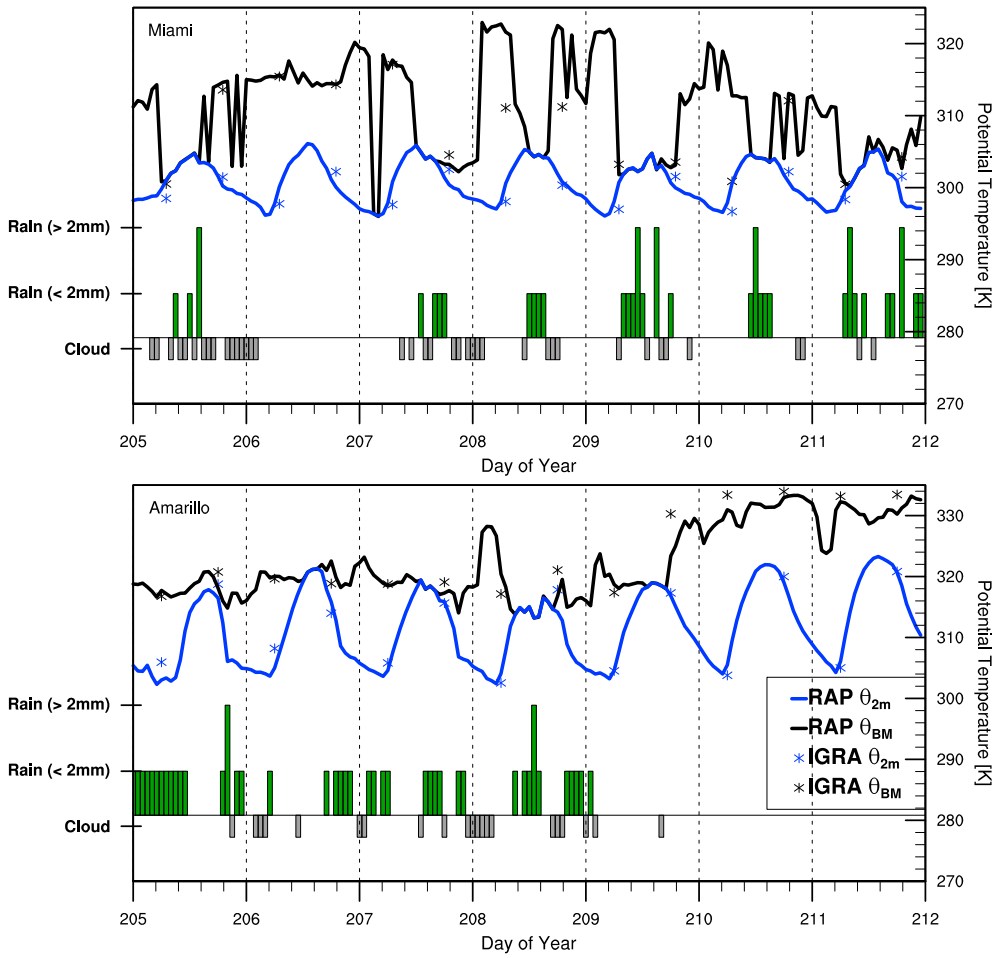

Figure 2. Hourly buoyant mixing potential temperature, θ_{BM}, from RAP (black line) and IGRA soundings (black asterisk) compared against hourly 2 m potential temperature from RAP (blue line) and first sounding level potential temperature from IGRA (blue asterisk) from 23 July to 30 July 2012 for Miami, Florida (25.75°N and 80.83°W), and Amarillo, Texas (35.23°N and 101.70°W). RAP precipitation (green bars) is binned by hourly accumulations greater than 2 mm and less than 2 mm. Grey bars represent the presence of nonprecipitating clouds lower than 8 km above the ground also from RAP. Stations are identified in Figure 3.

January 1970 to June 2013 where available. To be used, each sounding must have at least eight levels with 60% soundings for a station recording more than 20 levels. Additionally, soundings are filtered to include only those that reach 600 hPa to ensure sufficient vertical resolution when calculating the HCF variables. Finally, stations must have at least 500 soundings to be included in the climatological analysis (section 4.2).

3.2. Rapid Refresh

[10] One week of output (23 July to 30 July 2012) from the Rapid Refresh (RAP) forecast model system, the next generation of the Rapid Update Cycle [*Benjamin et al.*, 2004], is used to illustrate the utility of the HCF on hourly timescales. RAP is an operational short-range weather forecast system using the regional Weather Research and Forecast model (WRF-Advanced Research version 3.3) [*Skamarock et al.*, 2008] to produce hourly forecasts over North America. The RAP model has 50 vertical levels up to 10 hPa and a horizontal grid spacing of 13 km. Here we use output from the first forecast hour providing a close representation of the assimilated observations. Instantaneous vertical profiles of temperature, specific humidity, and cloud cover are used, in addition to total accumulated precipitation over the prior hour.

4. Results

4.1. Event Application of HCF

[11] A maritime (Miami, Florida) radiosonde station and a continental (Amarillo, Texas) radiosonde station are examined for a week in July spanning days of year (DOY) 205–212 (Figure 2). Miami and Amarillo are among the stations in Figure 3. The θ_{2m} is compared against θ_{BM} instead of comparing the BCL and PBL heights to avoid uncertainties regarding definition and calculation of boundary layer height [*Seidel et al.*, 2010; *LeMone et al.*, 2013]. Note that the θ_{BM}-θ_{2m} comparison provides the same information regarding the departure from saturation as the BCL-PBL comparison except in a different parameter space.

[12] Although Miami and Amarillo represent two distinct climate regimes, at both stations, precipitation and cloud cover are absent on days when daytime θ_{BM} is much larger than θ_{2m} (Figure 2). Further, θ_{BM} calculated from RAP is shown to closely follow θ_{BM} calculated from morning (1200 UTC) and afternoon (0000 UTC) IGRA observations, providing confidence in the hourly RAP output (Figure 2). For Miami, θ_{BM} shows strong diurnal variations with a minimum of 300 K, typically during midmorning, and a maximum at night

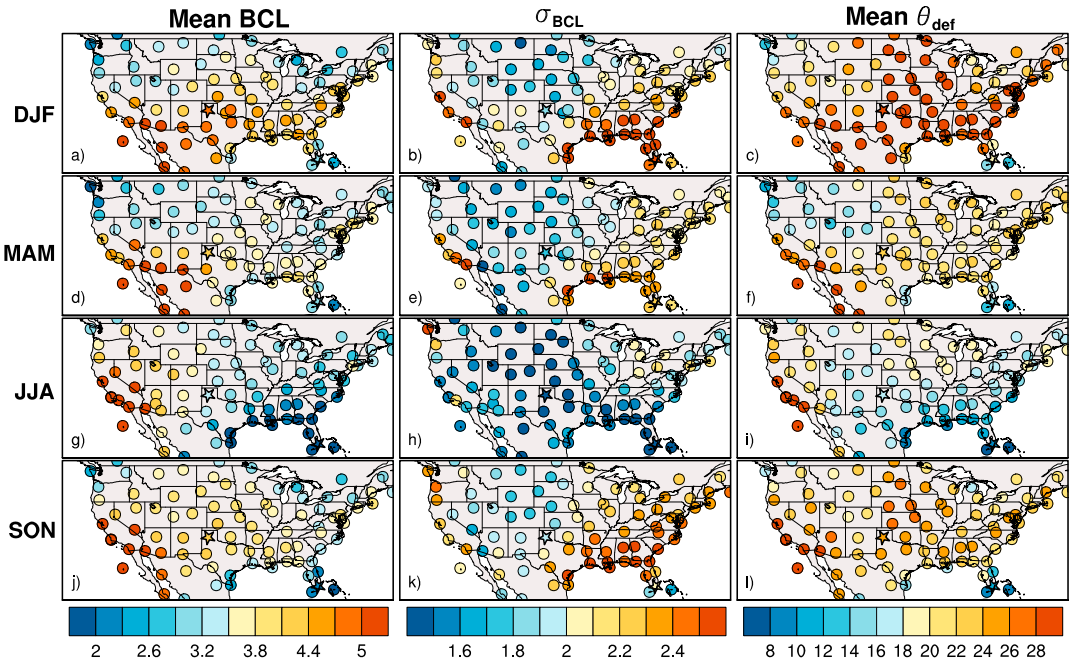

Figure 3. (left) Seasonal cycle of average buoyant condensation level (BCL in km), (middle) intraseasonal variability of the BCL (σ_{BCL} in km), and (right) average additional temperature increase necessary to trigger convection (θ_{def} in K) at IGRA stations for 1200 UTC soundings. The stars represent the Amarillo, Texas, and Miami, Florida, stations.

greater than 310 K. This suggests that there is a strong diurnal change in low-level moisture consistent with a land-sea breeze (see supporting information for further discussion of the Miami land-sea breeze.) Convection appears to be controlled by the rapid daytime decrease of θ_{BM} (e.g., moistening of the large-scale background state and lowering BCL height) during this week.

[13] At Amarillo, there is little diurnal variability in θ_{BM}, suggesting that the atmospheric background state is not largely influenced by local surface forcing during this week (Figure 2). Additionally, θ_{BM} rapidly increases during the evening of DOY 209, during which time clear-sky conditions persist. This increase in θ_{BM} occurred when a ridge developed over the central U.S. producing an upper level high-pressure system centered over northern Texas (see supporting information for further discussion.) However, there are times when clouds and precipitation occur without a θ_{BM}-θ_{2m} intersection, namely at night for DOY 205–209. Because the HCF is developed to diagnose convective triggering due to surface heating, nocturnal precipitation events associated with eastward propagating mesoscale convective complexes [*Moncrieff*, 2013] over the central U.S. likely would not influence θ_{BM} unless near-surface vertical profiles of q and θ were impacted. This is discussed further in section 5. Overall, we see the ability of the HCF to capture the background atmospheric state for nonprecipitating transient synoptic systems (Amarillo high pressure system) and changes in mesoscale circulation (Miami land-sea breeze.)

4.2. BCL Height Climatology

[14] The mean and standard deviations of the BCL height are presented by season over the U.S., using several decades of 1200 UTC IGRA data (Figure 3). The lowest BCL heights occur over the Southeastern U.S., and the highest values are over the Southwestern U.S. during the summer months (June-July-August (JJA)) with a gradual transition from low to high values moving westward. The seasonal cycle of average BCL height is strongest in the southern half of the U.S. and east of the Rocky Mountains with a winter (December-January-February (DJF)) maximum between 3.8 and 5 km and a summer (JJA) minimum of 1.5 and 3.5 km. This is expected because convective activity typically peaks during the summer months. Conversely, the seasonal cycle for the northwest U.S. is weaker and has the lowest BCL heights in DJF and highest in JJA. The Southwest shows almost no seasonal variation in BCL height (Figure 3).

[15] The pattern of BCL height variability (σ_{BCL}) does not change from fall (September-October-November) through spring (March-April-May). However, there is a strong reduction in variability that occurs during JJA from the Southeast Coast through the Plains and Rocky Mountains (Figure 3). Furthermore, σ_{BCL} has the most pronounced seasonal cycle over the Southeast Coast with the BCL height varying by more than 2.5 km from day-to-day in DJF and less than 1.5 km in JJA.

[16] Considering the seasonal behavior of BCL height, locations where the land surface may play a role in triggering convection can be deduced and highlighted for further investigation. Focusing on JJA, the BCL height patterns can be qualitatively separated into three categories: areas where the BCL height is (1) low, making convection likely under most surface (soil moisture) conditions, (2) attainable under specific surface conditions making convection conditional on the land surface state, and (3) so high as to make moist convection unattainable. Note that these categories mirror the land-atmosphere regimes described by *Findell and Eltahir* [2003]; however, the BCL height has the advantage of summarizing the background state in a single metric without requiring the selection of arbitrary humidity or stability levels making the BCL height (or θ_{BM}) more globally applicable.

[17] To provide an examination of the likelihood of convective triggering, the average θ_{def} is also presented (Figure 3), where smaller values represent a greater chance of triggering. The seasonal cycle is amplified when presented in terms of θ_{def}, with DJF requiring an increase of more than 28 K from the morning θ_{2m} (1200 UTC) on average for most of the U.S. and less than 18 K for JJA (Figure 3). As a first approximation for identifying the three regimes, terciles of the average θ_{def} across all stations and seasons were calculated, where values less than 16 K (~33rd percentile) represent the first regime, values between 16 and 23 K represent the second regime, and values greater than 23 K (~67th percentile) represent the third. The Southeast and Gulf Coasts would likely fall under the first regime because an increase in surface potential temperature of less than 16 K is required on average to trigger convection for JJA. The West Coast would lie in the third regime (convection unattainable over any surface) because morning (1200 UTC) θ_{2m} would need to increase by more than 23 K to trigger convection. The Central Plains, typically identified as a land-atmosphere coupling hotspot [*Koster et al*., 2006], and the Great Lakes region fall into the second regime, suggesting that convection may be favored if there is a sustained moisture source (through low-level moisture convergence or evapotranspiration) into the PBL or the surface is sufficiently dry, making it capable of overcoming the 16–23 K temperature deficit (Figure 3). Station-specific parameters that influence the diurnal temperature range (such as vegetation type, soil moisture, and soil properties) could influence the boundary between the three regimes. To more rigorously categorize these regimes, the diurnal evolution of θ_{def} must be examined. However, IGRA observations do not provide sufficient hourly resolution to perform this analysis.

5. Discussion and Conclusions

[18] A process-based diagnostic framework (HCF) is introduced to quantify the atmospheric background state within the context of land-boundary layer interactions. The HCF has advantages that make it useful for studying the impact of surface fluxes on convective triggering. First, the construction of the BCL height mimics the evolution of the convective boundary layer and initiation of convection to first order (Figure 1). Rather than lifting a hypothetical unmixed parcel, the HCF constructs a hypothetical boundary layer by incrementally inputting heat at the surface. Information regarding the atmospheric background state (via BCL height and θ_{BM}) and surface energy interaction can be derived (using θ_{def} and q_{def}) that are physically consistent with PBL development. The BCL height and θ_{BM} are diagnostic properties of a given profile not subject to parcel selection bias. The BCL is similar to the mixing condensation level (MCL), which has long been used for examining fog [*Petterssen*, 1939] and marine stratocumulus [*Miller et al*., 1998]. The primary difference is that the MCL assumes wind-driven mixing of both the θ and q profiles, whereas the BCL assumes buoyancy-driven mixing by perturbing θ_{2m} and mixing the q profile. An analogy could also be drawn with the convective condensation level (CCL); however, like the LCL, the CCL is calculated by lifting a parcel of water vapor that does not mix with its surroundings, resulting in the same shortcomings discussed above.

[19] Another advantage is that an atmospheric background state can be calculated during any time of day (Figure 2) or year (Figure 3). This allows for the evaluation of land-atmosphere coupling on an hourly basis without having to remove weather variability by time-averaging [cf., *Betts*, 2004; *Guo et al*., 2006; *Koster et al*., 2006]. The HCF may be easily applied because only temperature and humidity profiles are required. The sensitivity of the HCF to vertical resolution needs to be examined further; however, preliminary analysis shows that mean BCL height changes by less than +/−500 m for 75% of 1200 UTC soundings when the number of IGRA vertical levels are halved. Additionally, when analyzing 1200 UTC soundings BCL height climatology (Figure 3), the difference in solar time across the U.S. introduces biases of less than 160 m for most stations when using hourly RAP output from July 2012.

[20] Similar to other column-derived metrics [*De Ridder*, 1997; *Findell and Eltahir*, 2003], a primary shortcoming of HCF is its inability to distinguish between transient and locally driven precipitation. Although it was shown to capture low-level moisture advection (Figure 2), a passing precipitation event may rapidly lower the BCL height through reevaporation of precipitation within the PBL. This makes the signal between reevaporation and rapid low-level moisture convergence difficult to determine without subhourly profiles or information of surrounding synoptic conditions. Therefore, although the evolution of the atmospheric background state is accurately captured, more information would be required to identify the specific process. Combining BCL information with existing coupling diagnostics, such as the LCL deficit representation of near-surface parcel forcing [*Santanello et al*., 2011], may help identify the role of the land surface in triggering and enhancing convection.

[21] **Acknowledgments.** This work was supported by National Science Foundation grant 0947837 for Earth System Modeling post-docs. We would like to thank Bert Holtslag, Kirsten Findell, Craig Ferguson, Chiel van Heerwaarden, Alan Betts, Pierre Gentine, Randal Koster, Joseph Santanello, and Michael Ek for their helpful comments that have truly improved the quality of this manuscript.

[22] The Editor thanks Craig Ferguson and an anonymous reviewer for assistance evaluating this manuscript.

References

Benjamin, S. G., et al. (2004), An hourly assimilation forecast cycle: The RUC, *Mon. Weather Rev.*, *132*, 495, doi:10.1175/1520-0493(2004)132<0495:AHACTR>2.0.CO;2.

Berg, L. K., and R. B. Stull (2004), Parameterization of joint frequency distributions of potential temperature and water vapor mixing ratio in the daytime convective boundary layer, *J. Atmos. Sci.*, *61*(7), 813–828, doi:10.1175/1520-0469(2004)061<0813:POJFDO>2.0.CO;2.

Betts, A. K. (2000), Idealized model for equilibrium boundary layer over land, *J. Hydrometeorol.*, *1*(6), 507–523, doi:10.1175/1525-7541(2000)001<0507:IMFEBL>2.0.CO;2.

Betts, A. K. (2004), Understanding hydrometeorology using global models, *Bull. Am. Meteorol. Soc.*, *85*(11), 1673–1688, doi:10.1175/BAMS-85-11-1673.

Betts, A. K. (2009), Land-surface-atmosphere coupling in observations and models, *J. Adv. Model. Earth Syst.*, *2*, doi:10.3894/JAMES.2009.1.4. [online] Available from: http://james.agu.org/index.php/JAMES/article/view/v1n4 (Accessed 13 September 2012)

De Ridder, K. (1997), Land surface processes and the potential for convective precipitation, *J. Geophys. Res.*, *102*(D25), 30,085–30,090, doi:10.1029/97JD02624.

Dirmeyer, P. A. (2011), The terrestrial segment of soil moisture-climate coupling, *Geophys. Res. Lett.*, *38*, L16702, doi:10.1029/2011GL048268.

Durre, I., R. S. Vose, and D. B. Wuertz (2006), Overview of the Integrated Global Radiosonde Archive, *J. Clim.*, *19*(1), 53–68, doi:10.1175/JCLI3594.1.

Ek, M. B., and A. A. M. Holtslag (2004), Influence of soil moisture on boundary layer cloud development, *J. Hydrometeorol.*, *5*(1), 86–99, doi:10.1175/1525-7541(2004)005<0086:IOSMOB>2.0.CO;2.

Fennessy, M. J., and J. Shukla (1999), Impact of initial soil wetness on seasonal atmospheric prediction, *J. Clim.*, *12*(11), 3167–3180, doi:10.1175/1520-0442(1999)012<3167:IOISWO>2.0.CO;2.

Ferguson, C. R., and E. F. Wood (2011), Observed land-atmosphere coupling from satellite remote sensing and reanalysis, *J. Hydrometeorol.*, *12*(6), 1221–1254, doi:10.1175/2011JHM1380.1.

Ferguson, C. R., E. F. Wood, and R. K. Vinukollu (2012), A global intercomparison of modeled and observed land-atmosphere coupling, *J. Hydrometeorol.*, *13*(3), 749–784, doi:10.1175/JHM-D-11-0119.1.

Findell, K. L., and E. A. B. Eltahir (2003), Atmospheric controls on soil moisture-boundary layer interactions. Part I: Framework development, *J. Hydrometeorol.*, *4*(3), 552–569, doi:10.1175/1525-7541(2003)004<0552:ACOSML>2.0.CO;2.

Findell, K. L., P. Gentine, B. R. Lintner, and C. Kerr (2011), Probability of afternoon precipitation in eastern United States and Mexico enhanced by high evaporation, *Nat. Geosci.*, *4*(7), 434–439, doi:10.1038/ngeo1174.

Gentine, P., A. K. Betts, B. R. Lintner, K. L. Findell, C. C. van Heerwaarden, and F. D'Andrea (2013a), A probabilistic bulk model of coupled mixed layer and convection. Part II: Shallow convection case, *J. Atmos. Sci.*, *70*(6), 1557–1576, doi:10.1175/JAS-D-12-0146.1.

Gentine, P., A. A. M. Holtslag, F. D'Andrea, and M. Ek (2013b), Surface and atmospheric controls on the onset of moist convection over land, *J. Hydrometeorol.*, *14*, 1443–1462, doi:10.1175/JHM-D-12-0137.1.

Guichard, F., et al. (2004), Modelling the diurnal cycle of deep precipitating convection over land with cloud-resolving models and single-column models, *Q. J. R. Meteorol. Soc.*, *130*(604), 3139–3172, doi:10.1256/qj.03.145.

Guo, Z., et al. (2006), GLACE: The global land-atmosphere coupling experiment. Part II: Analysis, *J. Hydrometeorol.*, *7*(4), 611–625, doi:10.1175/JHM511.1.

Guo, Z., P. A. Dirmeyer, and T. DelSole (2011), Land surface impacts on subseasonal and seasonal predictability, *Geophys. Res. Lett.*, *38*, L24812, doi:10.1029/2011GL049945.

Haiden, T. (1997), An analytical study of cumulus onset, *Q. J. R. Meteorol. Soc.*, *123*(543), 1945–1960, doi:10.1002/qj.49712354309.

Koster, R. D., et al. (2006), GLACE: The global land-atmosphere coupling experiment. Part I: Overview, *J. Hydrometeorol.*, *7*(4), 590–610, doi:10.1175/JHM510.1.

Koster, R. D., et al. (2011), The second phase of the global land-atmosphere coupling experiment: Soil moisture contributions to subseasonal forecast skill, *J. Hydrometeorol.*, *12*(5), 805–822, doi:10.1175/2011JHM1365.1.

LeMone, M. A., M. Tewari, F. Chen, and J. Dudhia (2013), Objectively determined fair-weather CBL depths in the ARW-WRF model and their comparison to CASES-97 observations, *Mon. Weather Rev.*, *141*(1), 30–54, doi:10.1175/MWR-D-12-00106.1.

Miller, M. A., M. P. Jensen, and E. E. Clothiaux (1998), Diurnal cloud and thermodynamic variations in the stratocumulus transition regime: A case study using in situ and remote sensors, *J. Atmos. Sci.*, *55*(13), 2294–2310, doi:10.1175/1520-0469(1998)055<2294:DCATVI>2.0.CO;2.

Moncrieff, M. W. (2013), The multiscale organization of moist convection and the intersection of weather and climate, in *Climate Dynamics: Why Does Climate Vary?*, edited by D.-Z. Sun and F. Bryan, pp. 3–26, AGU, Washington D. C., doi:10.1029/2008GM000838.

Petterssen, S. (1939), Some aspects of formation and dissipation of fog, *Geofys. Publ.*, *12*(10), 22.

Santanello, J. A., C. D. Peters-Lidard, S. V. Kumar, C. Alonge, and W.-K. Tao (2009), A modeling and observational framework for diagnosing local land-atmosphere coupling on diurnal time scales, *J. Hydrometeorol.*, *10*(3), 577–599, doi:10.1175/2009JHM1066.1.

Santanello, J. A., C. D. Peters-Lidard, and S. V. Kumar (2011), Diagnosing the sensitivity of local land-atmosphere coupling via the soil moisture-boundary layer interaction, *J. Hydrometeorol.*, *12*(5), 766–786, doi:10.1175/JHM-D-10-05014.1.

Santanello, J. A., C. D. Peters-Lidard, A. Kennedy, and S. V. Kumar (2013), Diagnosing the nature of land-atmosphere coupling: A case study of dry/wet extremes in the U.S. Southern Great Plains, *J. Hydrometeorol.*, *14*(1), 3–24, doi:10.1175/JHM-D-12-023.1.

Seidel, D. J., C. O. Ao, and K. Li (2010), Estimating climatological planetary boundary layer heights from radiosonde observations: Comparison of methods and uncertainty analysis, *J. Geophys. Res.*, *115*, D16113, doi:10.1029/2009JD013680.

Seneviratne, S. I., T. Corti, E. L. Davin, M. Hirschi, E. B. Jaeger, I. Lehner, B. Orlowsky, and A. J. Teuling (2010), Investigating soil moisture-climate interactions in a changing climate: A review, *Earth Sci. Rev.*, *99*(3–4), 125–161, doi:10.1016/j.earscirev.2010.02.004.

Skamarock, W. C., J. B. Klemp, J. Dudhia, D. O. Gill, D. M. Barker, M. G. Duda, X.-Y. Huang, W. Wang, and J. G. Powers (2008), A description of the advanced research WRF version 3, *NCAR Tech. Note*, *NCAR/TN–475+STR*.

Van Heerwaarden, C. C., J. Vilà-Guerau de Arellano, A. Gounou, F. Guichard, and F. Couvreux (2010), Understanding the daily cycle of evapotranspiration: A method to quantify the influence of forcings and feedbacks, *J. Hydrometeorol.*, *11*(6), 1405–1422, doi:10.1175/2010JHM1272.1.

Zhang, Y., and S. A. Klein (2010), Mechanisms affecting the transition from shallow to deep convection over land: Inferences from observations of the diurnal cycle collected at the ARM Southern Great Plains site, *J. Atmos. Sci.*, *67*(9), 2943–2959, doi:10.1175/2010JAS3366.1.

Zhang, Y., and S. A. Klein (2013), Factors controlling the vertical extent of fair-weather shallow cumulus clouds over land: Investigation of diurnal-cycle observations collected at the ARM Southern Great Plains Site, *J. Atmos. Sci.*, *70*(4), 1297–1315, doi:10.1175/JAS-D-12-0131.1.